

## Supplemental Figures

Figure S1. Characterization of E100K mutation in GCL, Related to Figure 1

Figure S2. Purification of GCL-interacting protein complexes from *Drosophila* embryo lysates, Related to Figure 2

Figure S3. Assessment of the conserved GCL domain, Related to Figure 3

Figure S4. *gcl*, *tsl* double mutant embryos have no apparent defects in PGC formation including centrosome positioning, but accumulate Torso protein and show phenotypes associated with the defects in the Torso signaling pathway, Related to Figure 4

Figure S5. The canonical Torso signaling pathway components do not inhibit PGC formation, Related to Figure 4

Figure S6. Assessment of Torso<sup>Deg</sup> mutant, Related to Figure 5

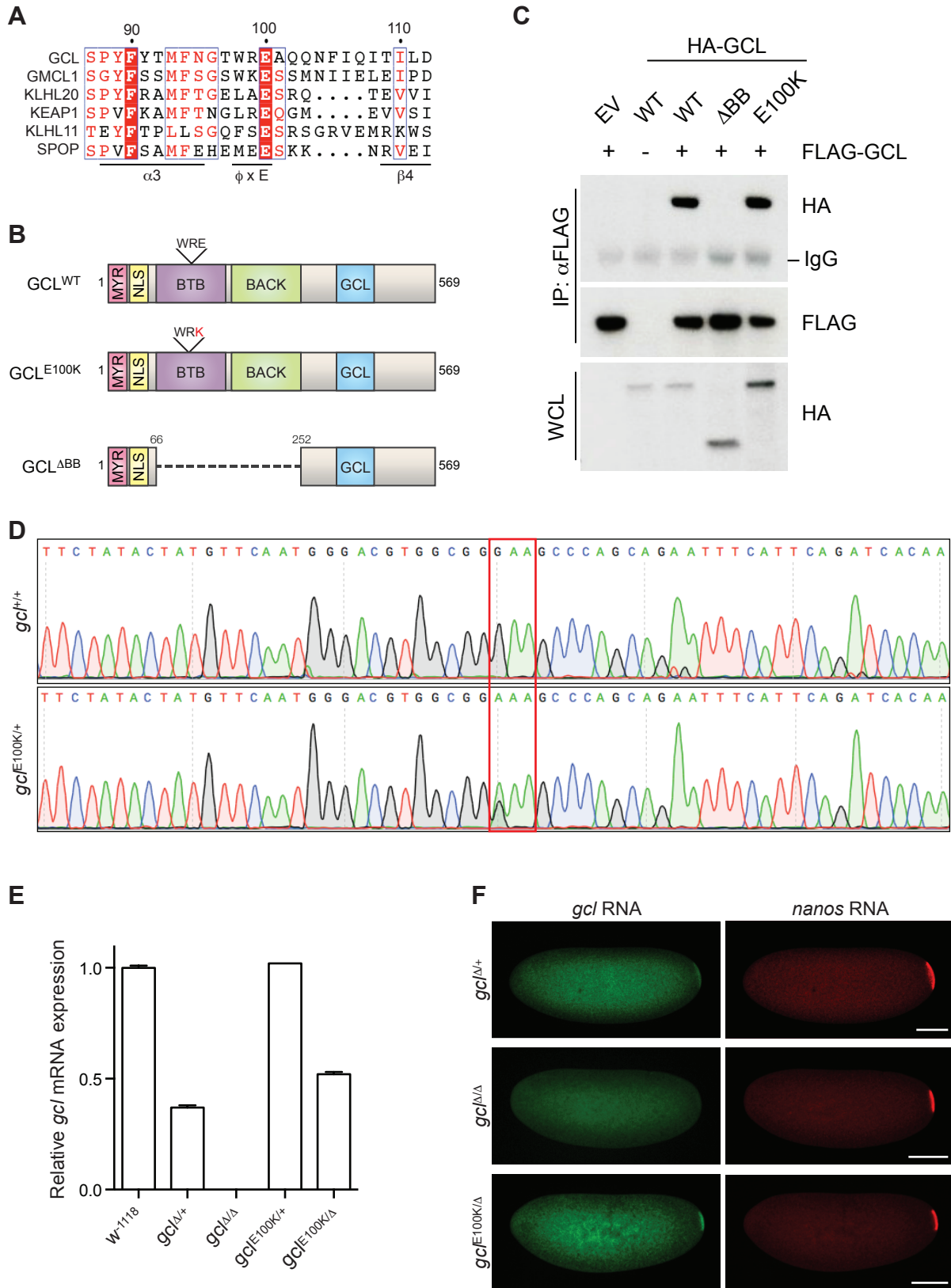


Figure S1 (See legend on next page)

**Figure S1. Characterization of E100K mutation in GCL, Related to Figure 1**

(A) Sequence alignment of the  $\phi$ -x-E motif found in *Drosophila* GCL, its human homolog GMCL1, and other BTB-domain substrate adaptors of CRL3. White letters/red background and red letters indicate identity and similarity, respectively. Numbers indicate the residue position in the *Drosophila* protein sequence.

(B) Construct cartoon. Amino acid change within the  $\phi$ -x-E motif (WRE) indicated in red.

(C) *Drosophila* Schneider 2 (S2) cells were co-transfected with constructs encoding FLAG-tagged GCL and HA-tagged GCL variants (WT,  $\Delta$ BB, or E100K) or empty vector (EV), as indicated. Cell lysates were immunoprecipitated (IP) with anti-FLAG resin, and immunocomplexes probed with indicated antibodies. HA-tagged GCL<sup>WT</sup> and GCL<sup>E100K</sup>, but not GCL <sup>$\Delta$ BB</sup>, can dimerize with FLAG-tagged GCL<sup>WT</sup>.

(D) Sequencing and trace results of the EMS-induced *gcl* mutation show GAA (Glutamic acid) to AAA (Lysine) substitution in comparison to wild-type control.

(E) Oocytes of indicated genotype were dissected, and *gcl* mRNA level was analyzed by qRT-PCR (mean of 3 technical replicates  $\pm$  standard deviation).

(F) Posterior enrichment of *gcl* and *nanos* RNAs were detected by RNA FISH. Scale bar = 100 $\mu$ m.

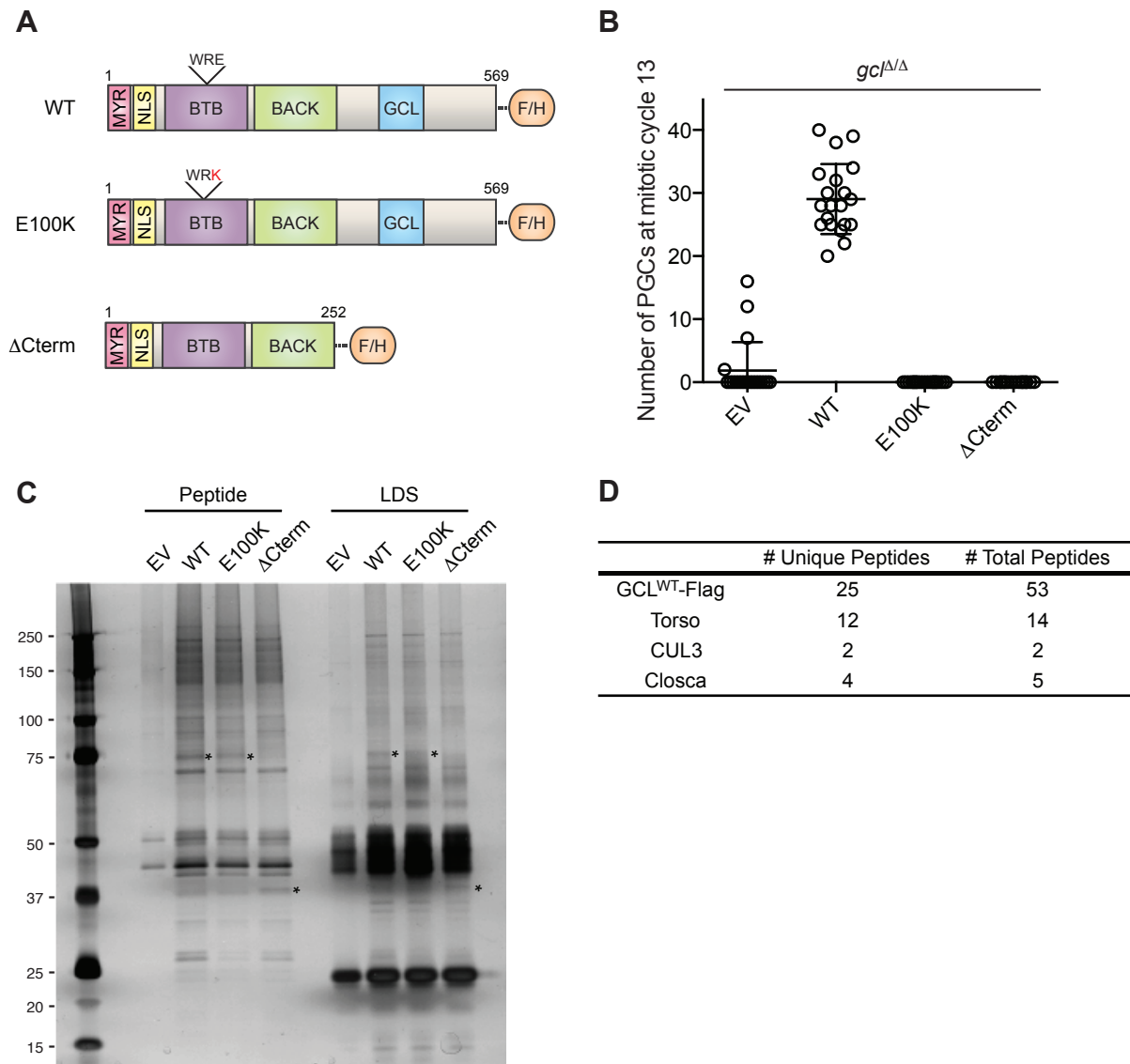


**Figure S2. Purification of GCL-interacting protein complexes from *Drosophila* embryo lysates, Related to Figure 2**

(A) Cartoon of constructs used for GCL complex purification.

(B) Number of PGCs in *gc1<sup>ΔΔ</sup>* embryos expressing either EV or a FLAG-HA-tagged GCL (WT, E100K, or  $\Delta$ Cterm) using the germline-specific *nanos-gal4::vp16* driver.

(C) Silver stain of GCL-bound protein complexes, eluted with either 3xFLAG peptides or LDS (Lithium Dodecyl Sulfate) as indicated. Asterisks indicate baits.

(D) Summary of mass spectrometry results. See also Table S1.

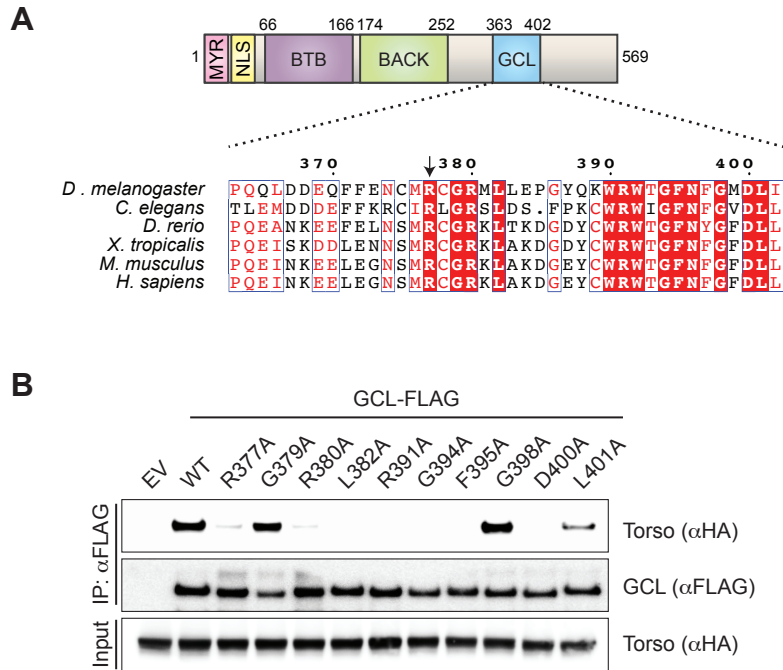


**Figure S3. Assessment of the conserved GCL domain, Related to Figure 3**

(A) Sequence alignment of GCL and its orthologs within the GCL domain. White letters/red background and red letters indicate identity and similarity, respectively. Numbers indicate the residue position in the *Drosophila* protein sequence.

(B) FLAG-tagged GCL variants with alanine substitution of the highly conserved residues within the GCL domain and HA-tagged Torso were in vitro translated and mixed together in 1:1 ratio. The mixture was immunoprecipitated (IP) with anti-FLAG resin, and immunocomplexes were probed with an antibody recognizing HA or FLAG. R377A was chosen for further functional tests shown in Fig 3.

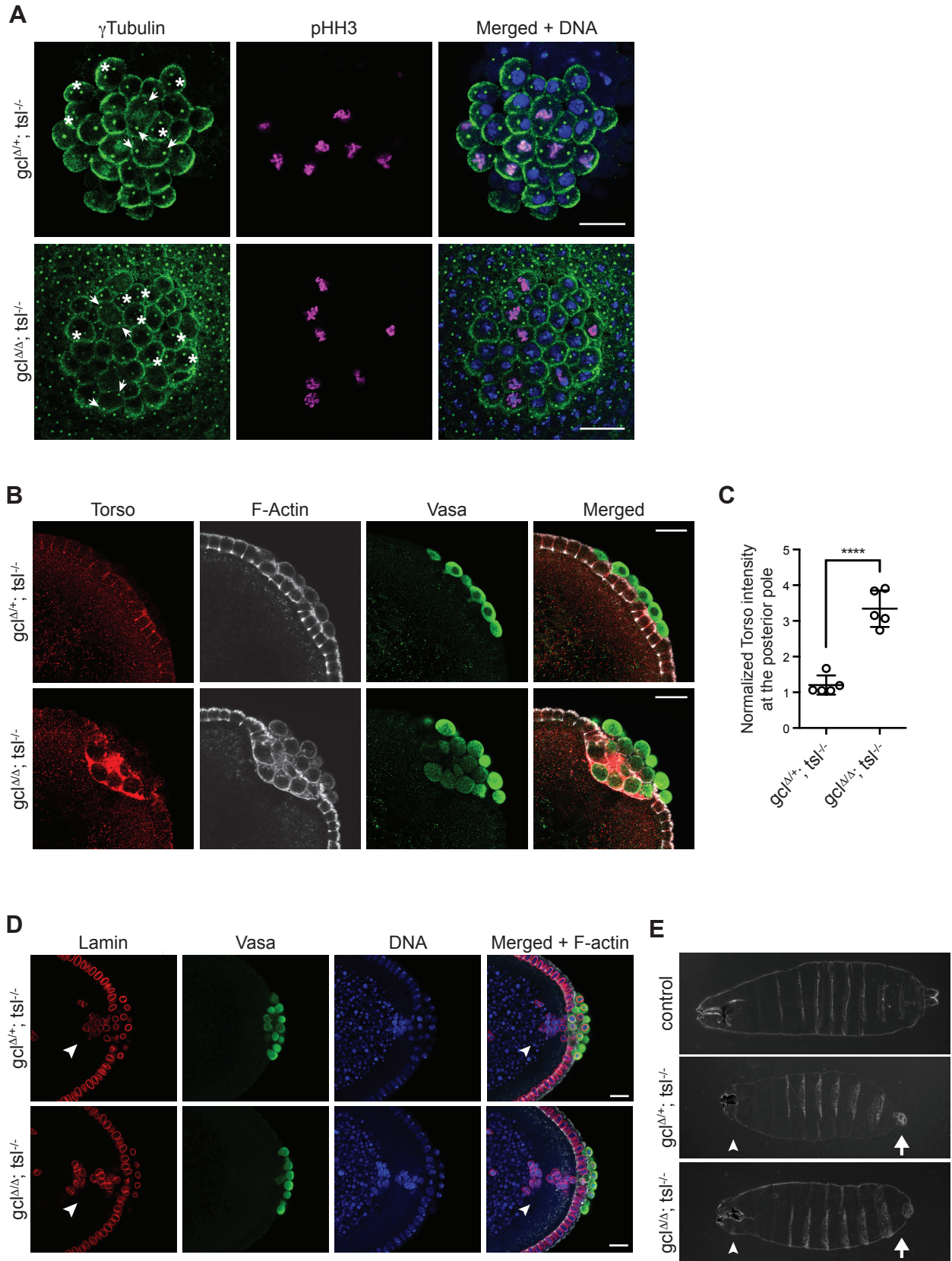


**Figure S4** (See legend on next page)

**Figure S4. *gcl*, *tsl* double mutant embryos have no apparent defects in PGC formation, including centrosome positioning, but accumulate Torso protein and show phenotypes associated with the defects in the Torso signaling pathway, Related to Figure 4**

(A) Fixed embryos from mothers of indicated genotype were immunostained with anti- $\gamma$ Tubulin (green) to visualize the centrosomes and anti-phospho Histone H3 Ser10 (pHH3, red) to mark the mitotic DNA. DNA (blue). To image a uniform layer of PGCs, posterior portion of the embryos was cut, turned, and mounted. Asterisks indicate the separating centrosomes in G2 phase. Arrows point at the centrosomes that are positioned at the opposite poles of the mitotic spindle during prometaphase. Scale bar = 20 $\mu$ m.

(B) Posterior pole of a representative embryo from mothers of the indicated genotypes. Fixed embryos were immunostained with anti-Torso (red) and anti-Vasa (green). F-actin (gray), DNA (blue).

(C) Torso signal intensity at the posterior pole of an individual embryo was quantified using ImageJ and normalized against the signal intensity at the dorsal end. (n=5, \*\*\*\*P > 0.0001).

(D) Fixed embryos from mothers of indicated genotype were immunostained with anti-LaminDm0 (red) and anti-Vasa (green). F-actin (gray), DNA (blue). Arrowheads point the nuclei falling into the yolk (known as the pole-hole phenotype seen in Torso pathway mutants). Scale bar=20 $\mu$ m

(E) Cuticle preparations of embryos from females of indicated genotype. Arrowheads indicate head skeleton defect, and arrows point to loss of terminal telson structures. *ts<sup>-/-</sup>* corresponds to *ts <sup>$\beta$ /4</sup>*. Wild-type flies (*w<sup>-1118</sup>*) were used as controls.

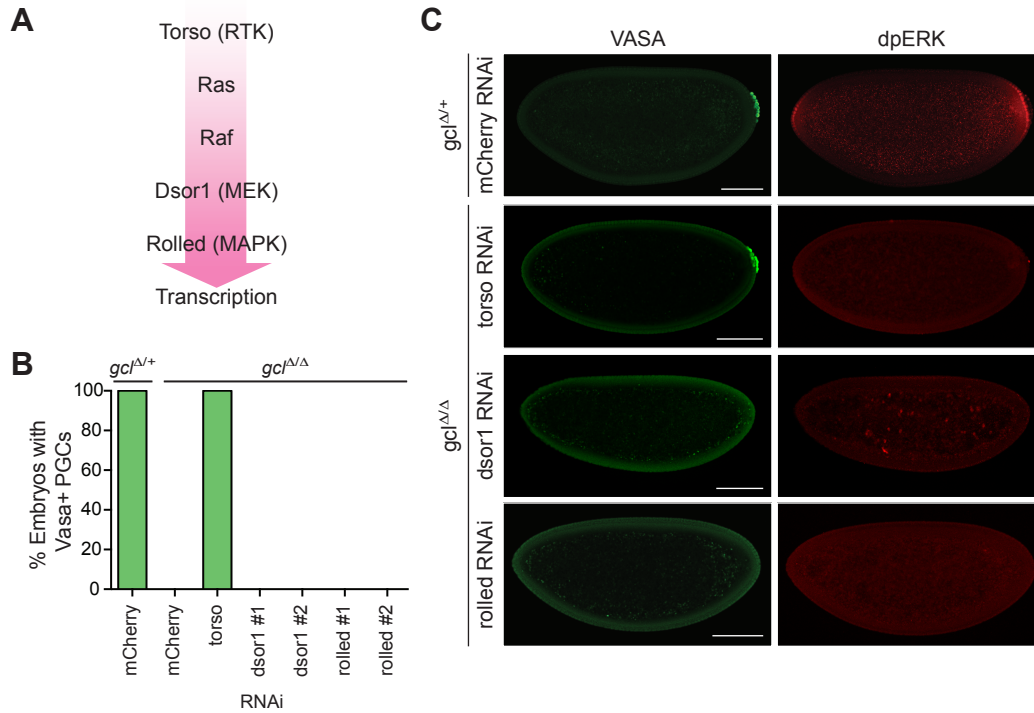


**Figure S5. The canonical Torso signaling pathway components do not inhibit PGC formation, Related to Figure 4**

(A) Summary of the canonical Torso signaling pathway leading to the transcriptional onset of the somatic terminal genes, such as *tll* and *hkb*.

(B) Dsor1 and Rolled, the canonical Torso signaling pathway components, were manipulated in *gcl<sup>Δ/Δ</sup>* embryos using transgenic-based in vivo knockdown (RNAi) with two individual shRNA constructs. RNAi against *mCherry* and *torso* in *gcl<sup>Δ/Δ</sup>* background were used as negative and positive control, respectively. Percentage of embryos with Vasa-positive PGCs was calculated and plotted. (n= 20 for each genotype)

(C) Representative RNAi embryos were fixed and immunostained with anti-Vasa (green) to visualize PGCs and anti-dpERK (red) to assess RNAi efficiency. Scale bar = 100 $\mu$ m.

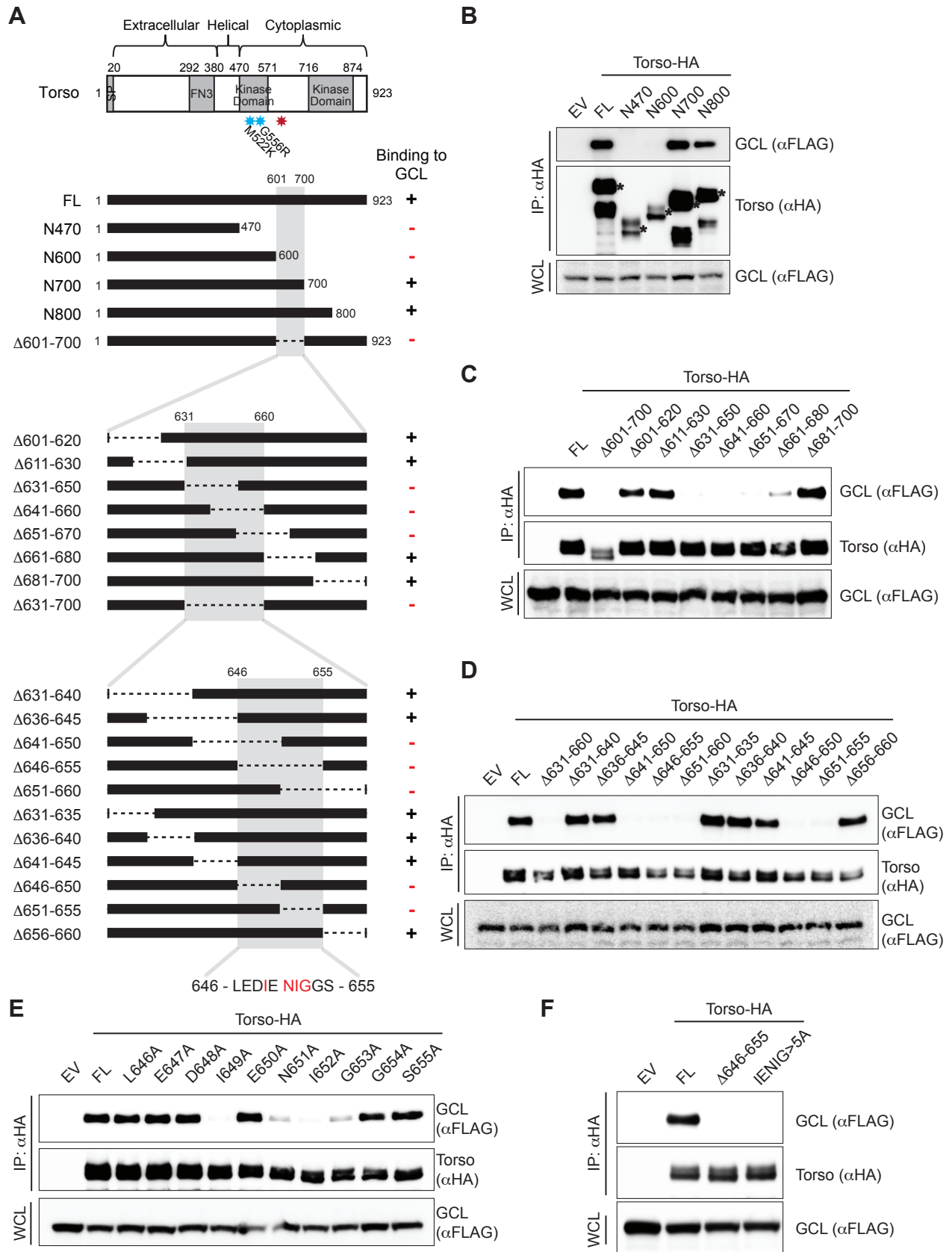


Figure S6 (See legend on next page)

**Figure S6. Assessment of Torso<sup>Deg</sup> mutant, Related to Figure 5**

(A) (Top) Domain architecture of Torso protein. The red asterisks indicate the degron motif between the split kinase domain identified in this study. The cyan asterisks indicate the position of the previously reported missense mutations, M522K and G556R (corresponding to the original alleles *torso<sup>WK</sup>* and *torso<sup>HH</sup>* respectively), within the first of the split kinase domains used in this study as loss-of-function mutants. (Bottom) Schematic representation of Torso truncation and deletion mutants generated to identify the degron motif. Binding of Torso to GCL is indicated with the symbol + (binding) or – (no binding). The light gray box indicates the binding region deduced from each set of immunoprecipitations performed in panels B-D. The four essential amino acids are indicated in red. To generate the minimal degron mutant Torso (Torso<sup>Deg</sup>), amino acids IENIG were mutated to a series of alanines (IENIG>5A). (B-F) HEK293T cells were transfected with FLAG-tagged GCL and either empty vector (EV) or the indicated Torso mutant construct. NLS mutant variant of GCL was used to enhance the interaction between GCL and Torso (see main text). Twenty-four hours post-transfection, cells were treated with MLN4924 for 3 hours, harvested, and lysed. Cell lysates were immunoprecipitated (IP) with anti-HA resin, and immunocomplexes were probed with FLAG or HA antibody. The asterisks indicate the baits.